

CEBAF-PR-86-013 VWC3  
F. Gross  
CEBAF Scientific Program  
\* 02059200094182  
  
B02059200094182B  
CEBAF-PR-86-013

**CEBAF SCIENTIFIC PROGRAM**

Franz Gross  
Continuous Electron Beam Accelerator Facility  
12070 Jefferson Avenue  
Newport News, VA 23606  
and  
Department of Physics  
College of William and Mary  
Williamsburg, VA 23185

CEBAF Scientific Program

Franz Gross  
Continuous Electron Beam Accelerator Facility  
12070 Jefferson Avenue  
Newport News, VA 23606

and

Department of Physics  
College of William and Mary  
Williamsburg, VA 23185

1. Introduction and Popular Overview

The exciting challenge facing nuclear physicists in the years ahead is to understand precisely how nuclei and nuclear matter are built up out of quarks and gluons, nucleons and mesons, and to understand how the effective forces in nuclei arise from the fundamental strong forces describable by Quantum Chromodynamics (QCD) and the fundamental electroweak forces describable by the standard model. The nuclear physicist today finds himself in a situation similar to that of the condensed matter physicist; he knows the fundamental force laws and the basic constituents and seeks to explain the structure and behavior of macroscopic systems constructed from these elementary constituents. In both fields, the path to be followed to achieve such an understanding is far from clear. Knowing the fundamental force law is a significant advantage, but collective phenomena not immediately suggested by the basic force laws can be expected (such as superconductivity in condensed matter physics, and one pion exchange forces in nuclear physics) and a major experimental and theoretical program is needed to discover and understand these phenomena.

The principal scientific mission of CEBAF is to carry out these studies on cold (or normal) nuclear matter. The electron, with its penetrating point-like interaction is an ideal probe of cold nuclear matter; by independently varying the energy and three-momentum transferred by the virtual photon, it is possible to either leave

the cold nucleus undisturbed by the probe, or to highly excite it and study individual constituents which emerge from the interaction. The principle scientific mission of the relativistic heavy ion collider (RHIC), planned to be constructed at Brookhaven National Laboratory, is to carry out these studies on hot nuclear matter. By smashing two high energy heavy ions together, nuclear matter at high temperature and energy density is obtained, and it should be possible to create a plasma of quarks and gluons. With both facilities it will be possible to understand the behavior of nuclear matter under a wide variety of conditions. The need for both of these new facilities has been recognized by the Nuclear Science Advisory Committee (NSAC)<sup>1</sup>.

Specific experimental programs currently planned for CEBAF are addressed in detail in Part 2. In this section, issues which the CEBAF experimental and theoretical program is designed to address are discussed in broad popular terms. Among the questions which CEBAF will address are:

- How is the structure of the nucleon modified in the nuclear medium? Does the nucleon swell?
- What is the nature of two-nucleon subsystems in the nuclear medium? Are nucleon-nucleon correlations large? Are there important contributions from independent 6-quark channels which do not overlap the NN subspace (dibaryons)?
- What is the precise role of excited baryons in the nuclear medium? Specifically, what is the free baryon spectrum, and how important are these baryons to the structure of cold nuclei? How is the structure of  $N^*$ 's and  $\Lambda$ 's modified by the nuclear medium? What are the  $N^*-N$  and  $\Lambda$ -N forces?
- What is the role of strange and other heavy quarks in the nuclear medium?
- How are elementary process, such as e-p scattering modified by the nuclear medium? How do quarks hadronize in the nuclear medium?
- How can the dynamics of quark confinement be best described and modeled (solitons, bags, fluxtubes, potentials)? How is this confinement modified by the presence of other nucleons, such as occurs in the nuclear medium?

- What degrees of freedom are important to the description of the nuclear wave function at short distances (high momentum transfer), and how large are its high momentum components?
- What are the "smoking gun" signatures (if any) of new phenomena related to quark degrees of freedom in nuclei?

A broad program of both theoretical and experimental work will be necessary before many of these questions can be answered.

If there are new phenomena related to the underlying quark degrees of freedom, their appearances and importance can be expected to depend strongly on the effective quark confinement radius. When nucleons are far apart, their constituent quarks remain with the parent nucleon. In this case the nuclear force is transmitted by the pion, a collective mechanism not currently understood in the language of QCD, and new phenomena related to the mingling of quarks should be absent. As nucleons are brought closer together, the confining forces may weaken, allowing the quarks to move from one nucleon to another, and new phenomena related to this mingling may occur. Clearly, the critical distance at which this happens will be related to the effective confinement radius of quarks inside of a nucleon.

Figure 1 shows three different views of the  ${}^4\text{He}$  nucleus, which are appropriate for different values of the confinement radius. In the first case, the confinement radius is large -- comparable to the radius of the nucleon itself. The meson cloud around the nucleon is absent, or very insignificant. Here the long range pion force still would play a role, but shorter range meson exchange forces would be replaced by quark interchange mechanisms. Signatures of explicit quark degrees of freedom should be visible even at comparatively low excitation energies and low momentum transfers, and the success of conventional nuclear models based on hadronic degrees of freedom with meson exchange would be an accident, or a consequence of duality (see below). This picture is suggested by the original MIT bag model<sup>2</sup>.

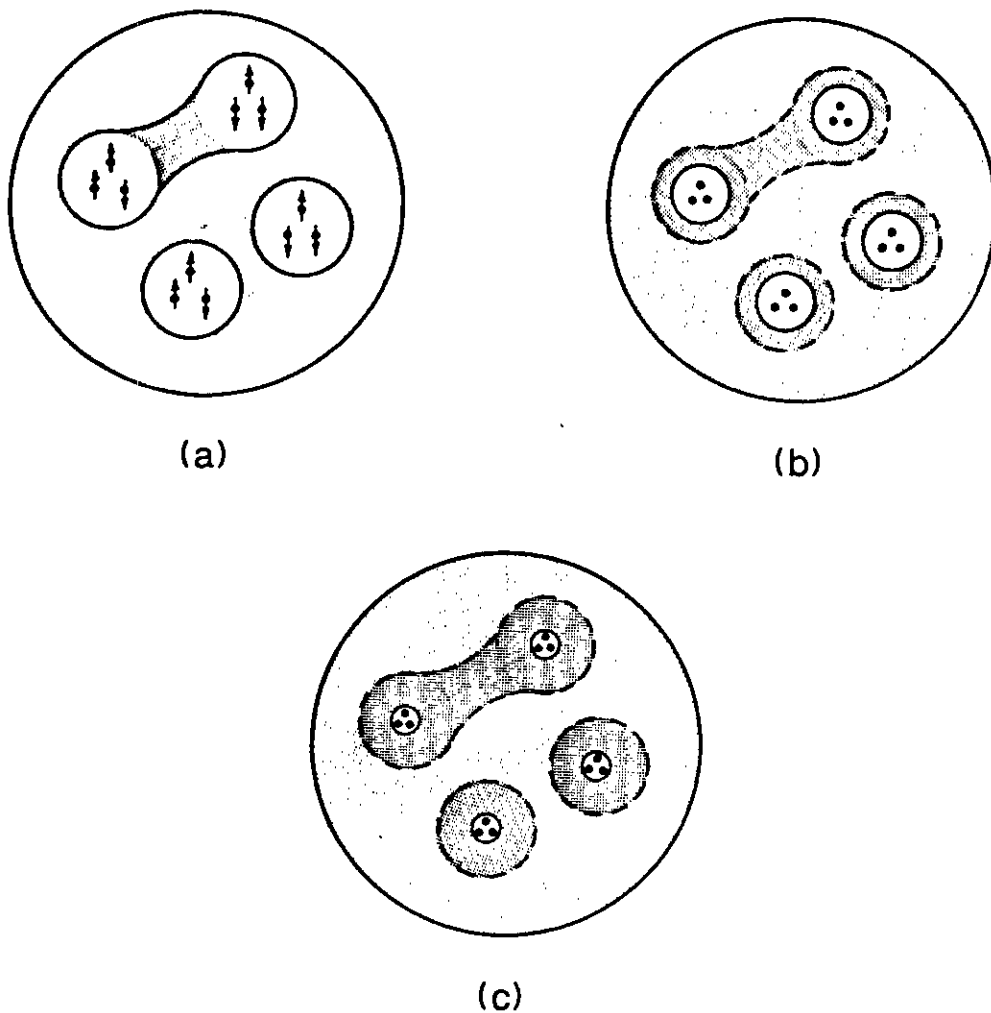


Figure 1 Cartoons of the  ${}^4\text{He}$  nucleus for different values of the effective confinement radius: (a) large (quarks occupy the entire volume of the nucleon), (b) intermediate (quark core with a thick meson "skin"), (c) small (nucleons are mostly mesons with a tiny quark core). Dark shading - pion (and other meson) clouds. Light shading - normal vacuum. White - QCD vacuum.

The other extreme possibility is that the confinement radius is very small, and that the nucleon is largely a meson cloud with the valence quarks confined inside of a tiny volume of nearly zero radius, as illustrated in Figure 1(c). This picture is suggested by the  $N_c \rightarrow \infty$  limit of QCD ( $N_c$  is the number of colors), in which, to lowest order in  $N_c^{-1}$ , baryons are built from topological soliton solutions of effective meson field equations<sup>3</sup>, such as the Skyrmion model<sup>4</sup>. It is also suggested by relativistic meson theory, in which the structure of the nucleon would arise primarily from its meson cloud. In this case, it is unlikely that effects from the quark core will be visible, and nuclear structure is likely to be fully understood in terms of meson interactions, with the possibility that non-linear meson interactions, such as those treated by Skyrmion models, will play a role.

Perhaps the most likely possibility is that the confinement radius will be intermediate in size, as illustrated in Figure 1(b). This picture is suggested by the cloudy bag model<sup>5</sup>, which has been quite successful phenomenologically. In this case, explicit effects from the quark core may appear only at the high momentum transfers which can be studied at CEBAF.

The previous discussion assumes that there are new phenomena related to quark degrees of freedom. It is possible that there are no smoking gun signatures, i.e. new phenomena which cannot be explained by meson theory. This would be the case if an exact duality between quark-gluon descriptions and meson-nucleon descriptions were to hold. That this might be the case is suggested by the observation<sup>6</sup> that any color singlet 6-quark state can be expressed in terms of a sum of states consisting of two color singlet 3-quark states. The three quark states in the sum may be highly deformed, corresponding to highly excited baryons, so that even in this case it could be more efficient to use a 6-quark basis consisting of a few states rather than a basis consisting of a large number of excited 3-quark baryons. But this observation raises the possibility that, if the number of meson and baryon states included

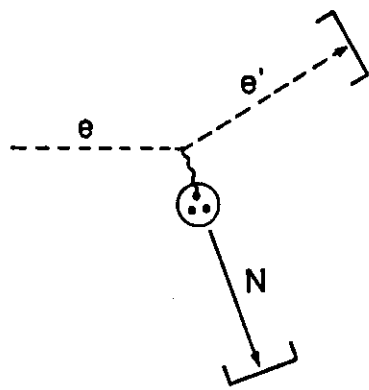
in a effective meson theory is enlarged sufficiently, it may be possible to describe all short range phenomena in terms of meson theory. Theoretical models which allow for this duality are needed.

While most of the questions raised in the beginning of this section will require considerably more thought before they can be formulated in sufficiently precise terms to be tested, the first three questions can be captured in a cartoon which will serve to give a popular focus to the CEBAF program. The cartoon, Figure 2, shows a  ${}^4\text{He}$  nucleus being probed by a high energy electron. At the moment it is being probed, it is in a state where one of its nucleons is swollen, one is in an excited  $\Delta$  or  $N^*$  state, and two have overlapped to form a 6-quark state. In Figure 2(b), the electron strikes one of the quarks in the swollen nucleon, knocking the nucleon from the nucleus. Both the electron and the nucleon are detected in an  $(e, e'N)$  experiment, and the cross section, when compared to that from a free nucleon (illustrated in Figure 2(a)) will reflect the altered charge distribution of the swollen nucleon. Alternatively, if the electron strikes the 6-quark state (Figure 2(c)), it could lead to an enhanced  $2N$  emission, which, if the two nucleons are highly correlated, could be detected in two spectrometers, one of which has a large acceptance. Finally, striking the  $\Delta$  or  $N^*$  (Figure 2(d)), could lead to a final  $2\pi N$  state, and all of these fragments can be detected in a Large Acceptance Spectrometer (LAS), with a nearly  $4\pi$  acceptance as shown. These three experiments can be thought of as typical of the programs to be carried out in the three experimental halls described in Section 3; each requires its own unique complement of experimental equipment.

## 2. Highlights of Experimental Programs Planned for CEBAF

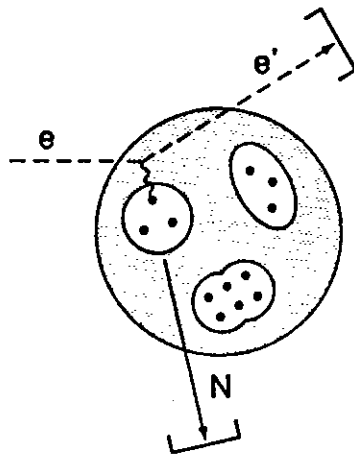
Highlights of seven experimental programs which have served to define the CEBAF experimental equipment will be discussed in this section. These are:

- Single nucleon emission -  $(e, e'N)$
- Two-nucleon emission -  $(e, e'2N)$

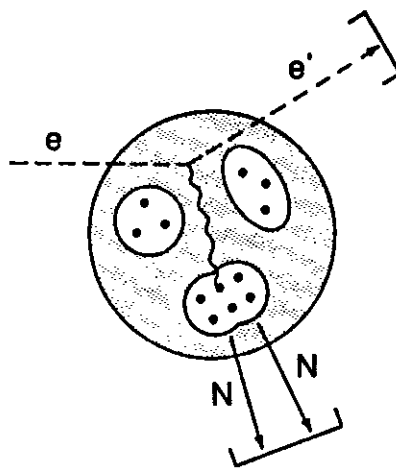


(a)

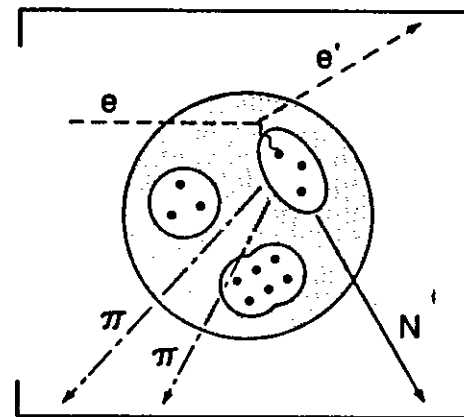
Figure 2 Cartoons representing electron scattering. In each case the electron emits a virtual photon which is absorbed by a quark. (a) Scattering from a free nucleon followed by detection of the outgoing electron and nucleon in coincidence. The other three figures all show scattering from  ${}^4\text{He}$ , with the electron striking different constituents. (b) The electron strikes a bound nucleon, swollen by the interactions with the nuclear medium, and the outgoing nucleon and electron are detected in coincidence. (c) The electron strikes a six-quark state, which emerges as two nucleons detected in coincidence with the electron. (d) The electron strikes an excited nucleon, which shatters into two pions and a nucleon, all of which are detected in a LAS.



(b)



(c)



(d)

- Study of excited baryons
- Hypernuclei - (e,e'K)
- Charge distribution of the neutron and deuteron
- Studies in the deep inelastic region
- Studies of the electroweak interaction

The first six of these programs were reviewed briefly in the RPAC report<sup>7</sup>; the latter has been discussed in the original SURA proposals<sup>8</sup>, and in the 1981 report of the Bates Study Group<sup>9</sup>. CEBAF contributors to RPAC include V. Burkert, F. Gross, B. Mecking, J. Mougey, and R.R. Whitney.

## 2.1 Single Nucleon Emission

The original motivation for measuring single nucleon emission in coincidence with electron scattering is that it could give a direct measurement of the square of the momentum space nuclear wave function, called the single particle density. As an introduction to coincidence measurements, and to see how this comes about, assume that meson exchange effects and final state interactions are small (this is often not the case -- see the discussion below). In this case, the electromagnetic interaction from the simplest nucleus, the deuteron, can be calculated from the two impulse approximation diagrams shown in Figure 3. If magnetic scattering is neglected (for simplicity) the differential cross section obtained from these diagrams is

$$\frac{d^5\sigma}{d\Omega dE' d\Omega_{p_1}} \simeq \sigma_M |F_p(Q^2)\psi(p_2^2) + F_n(Q^2)\psi(p_1^2)|^2 \quad (1)$$

where the scale of the overall interaction is set by the Mott cross section,

$$\sigma_M = \left( \frac{2\alpha E' \cos\theta/2}{Q^2} \right)^2, \quad (2)$$

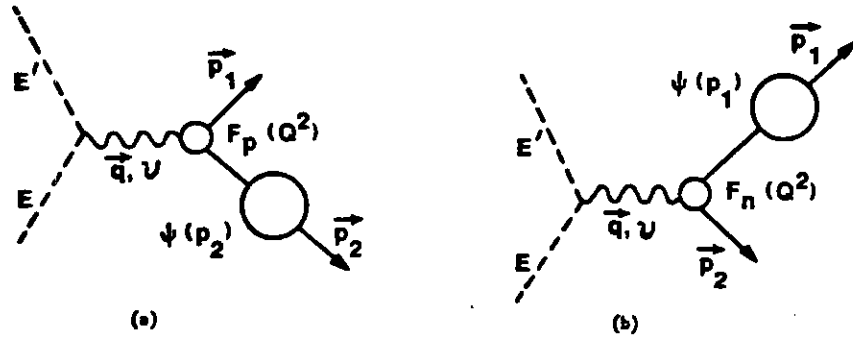


Figure 3 Impulse approximation diagrams for the  $d(e, e'p)$  experiment.

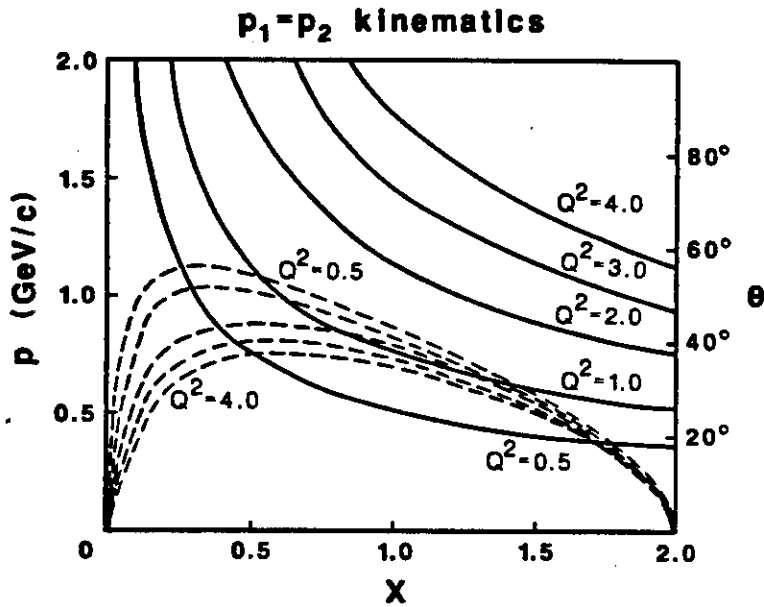


Figure 4 The dependence of nucleon momentum,  $p$ , and angle,  $\theta$  (equal to the angle between  $p_1$  and  $q$  -- also one-half the opening angle between the two nucleons), for the symmetric kinematics described in the text. The solid lines show the variation of  $p$  for constant  $Q^2$ , to be read using the scale on the left, and the dashed lines are  $\theta$ , to be read on the right.

with  $Q^2$  the 4-momentum transferred by the electron

$$Q^2 = q^2 - \nu^2 = 4EE' \sin^2 \frac{1}{2}\theta \quad , \quad (3)$$

$F_p(Q^2)$  and  $F_n(Q^2)$  are the form factors of the bound proton and neutron, respectively, and  $\psi$  is the wave function of the deuteron (which can be defined relativistically<sup>16</sup> by relating it to the d-n-p vertex function in a covariant way). To extract the square of the wave function from (1), it is helpful to choose symmetric kinematics so that  $|\vec{p}_1| = |\vec{p}_2| = p$ . Then

$$\frac{d^5\sigma}{d\Omega dE' d\Omega_p} \simeq \sigma_M |F_p(Q^2) + F_n(Q^2)|^2 |\psi(p^2)|^2 \quad . \quad (4)$$

By varying  $Q^2$  and the Bjorken scaling variable

$$x = \frac{Q^2}{2M\nu} \quad (5)$$

independently for this symmetric kinematics, it is possible to measure the  $p^2$  variation of this expression for a fixed  $Q^2$ , or the  $Q^2$  variation for a fixed  $p^2$ , as illustrated in Figure 4, and hence to measure the bound form factor dependence and wave function dependence independently.

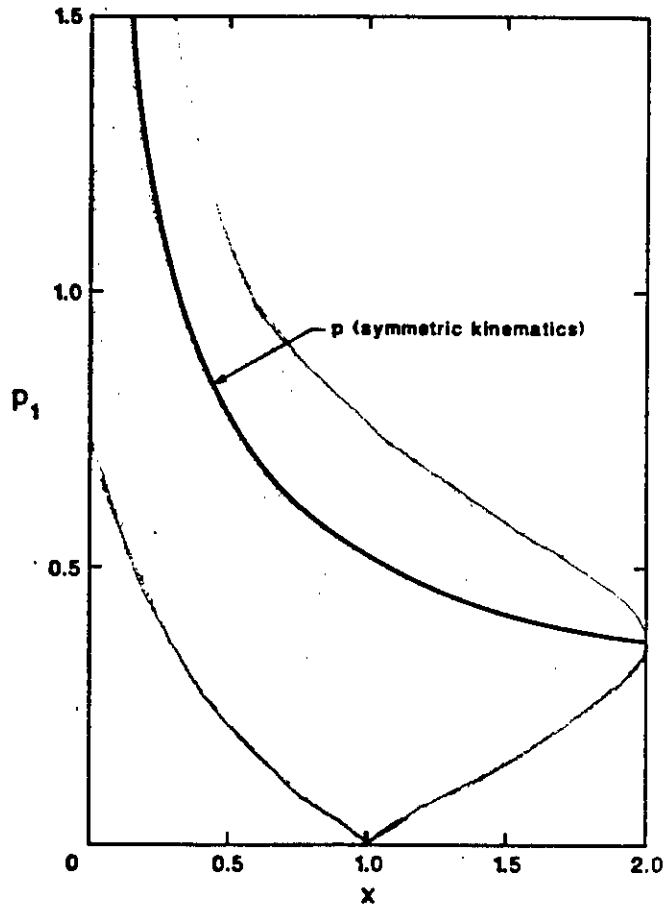
For comparison, the same simple theory gives the following expression for the single arm inclusive  $(e, e')$  cross section:

$$\frac{d^3\sigma}{d\Omega dE'} \simeq \sigma_M \int d\Omega_{p_1} |F_p(Q^2)\psi(p_2^2) + F_n(Q^2)\psi(p_1^2)|^2 \quad . \quad (6)$$

Since the outgoing nucleon is not detected, the cross section is dominated by that part of the region of integration where the wave function is the largest, which occurs for S states when the relative momentum is small. Figure 5 shows, for a fixed  $Q^2 = 0.5 \text{ (GeV/c)}^2$ , how the magnitude of  $\vec{p}$  varies as the integral over its direction

in Eq. 6 is carried out. Note that for all  $x \neq 2$ , values of  $|\vec{p}_1|$  occur which are considerably smaller than  $p$  given by symmetric kinematics. In particular, at the quasielastic peak, defined by the condition  $x = 1$ , the integral is dominated by contributions from regions where  $\vec{p}_1^2$  or  $\vec{p}_2^2 \approx 0$ , regardless of the value of  $Q^2$ . Coincidence experiments allow the experimenter to fix the momentum of the wave function at a particular value, and study the wave function in regions where it is small. In this way coincidence measurements give important new information not obtainable from single arm measurements.

Figure 5 Range of variation of  $|\vec{p}_1|$  (or  $|\vec{p}_2|$ ) under the integral in Eq. (6) for  $Q^2 = 0.5 \text{ (GeV/c)}^2$  and different values of  $x$ . For comparison, the value of  $p$  fixed by symmetric kinematics is also shown.



Recent high resolution measurements<sup>11</sup> of  $(e, e'p)$  from Pb at NIKHEF, give beautiful confirmation of the shell structure of nuclei (see Figure 6). A resolution  $\Delta E \approx 100 \text{ keV}$  was obtained in the experiments, permitting individual nuclear levels to be resolved. Other measurements from Saclay on the deuteron<sup>12</sup> and  $^3\text{He}$  (ref. 13) are shown in Figures 7, 8 and 9. The deuteron measurements are very

sensitive to the D state, and the  $^3\text{He}$  measurements show the potential this program has for giving detailed information about three body wave functions. Even studies of the few body system require high resolution; separation of the two- and three-body final states requires the resolution of  $\Delta E \approx 1$  MeV, obtained in this experiment and shown in Figure 8.

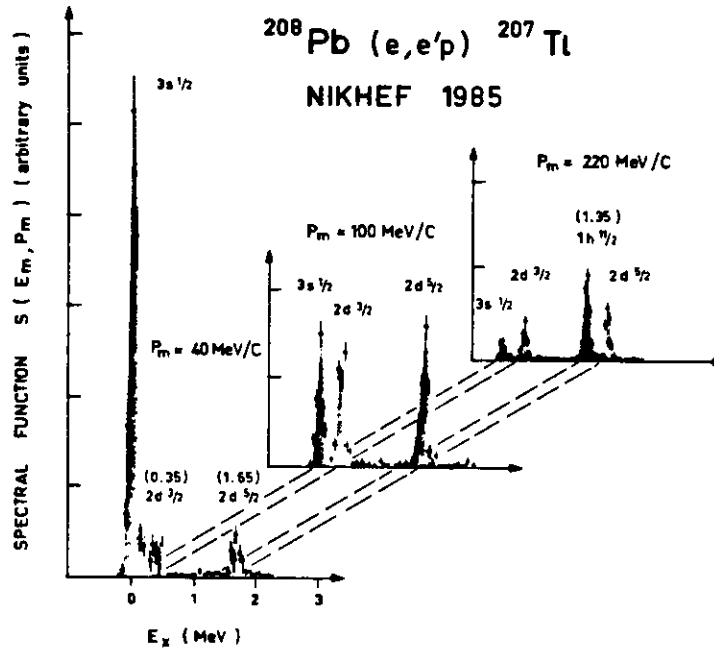
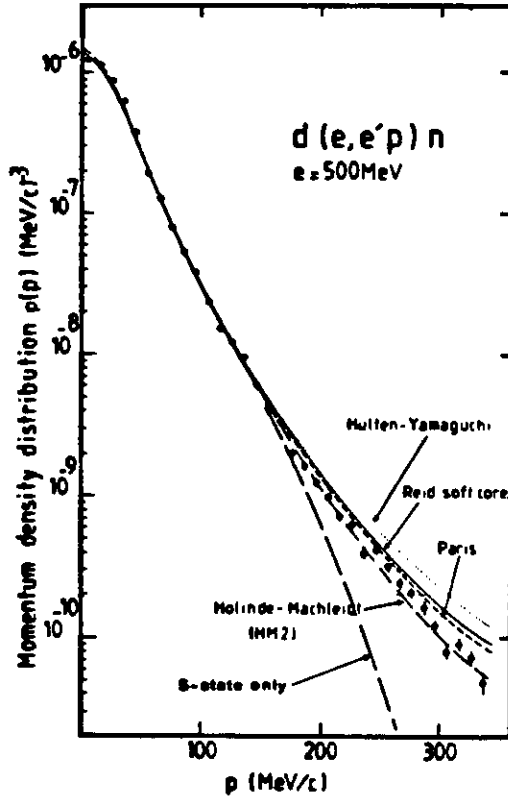


Figure 6 Recent NIKHEF data as plotted in Reference 11. High resolution permits different states of the final  $^{207}\text{Tl}$  nuclear system, corresponding to knockout of protons from different shells in the lead nucleus, to be distinguished.

In practice, final state interactions and meson exchange currents will make important contributions to the cross section, altering significantly the ease with which quantitative conclusions about the nuclear wave function can be extracted from these experiments. For example, Arenhovel<sup>14</sup> has shown that such effects vary from a few percent at  $p^2 \approx 0$  to 100% at  $p^2 \approx 300$  MeV for the deuteron measurements shown in Figure 7, and for other cases these effects can be considerably larger. This complicates the theoretical interpretations of these experiments and requires that

meson exchange effects, final state interactions, and contributions of the initial nuclear wave functions all be treated consistently.

Figure 7 Data from the Saclay measurement described in Ref. 12 compared with four theoretical models for the deuteron momentum density distribution. A dashed line showing the S-state contribution only, has been added to the figure.



At CEBAF, the  $(e, e'N)$  program will be extended to higher nucleon momenta  $p$  and higher momentum transfer  $Q^2$ , and the goal will be to study high momentum components of nuclear (especially few body) wave functions, study the three nucleon system fully and use such data to learn about 3 body forces, study the form factor of bound nucleons at high  $Q^2$  (to see if nucleons are swollen as discussed in Section 1), and to study neutron distributions through the  $(e, e'n)$  process. The latter cross sections are expected to be 10 times smaller than  $(e, e'p)$  cross sections, and are much harder to measure because of the inefficiency of neutron detectors, but are expected to be every bit as rewarding as the  $(e, e'p)$  program. They will require the full capability of CEBAF with its high current and high duty factor.

The general form of the  $(e, e'N)$  cross section has been given by Donnelly<sup>15</sup>. If the recoil polarization of the nucleon is

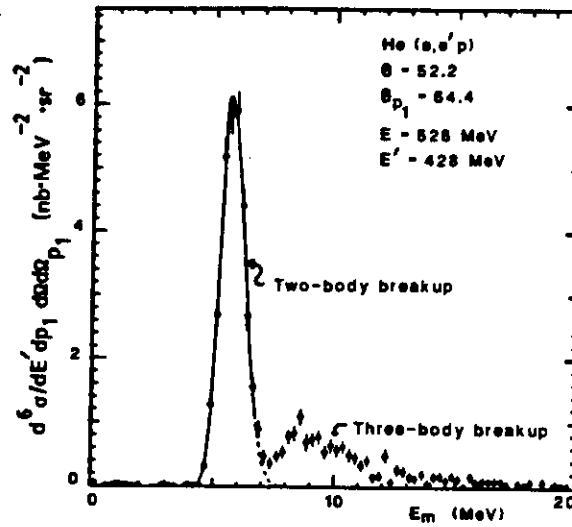


Figure 8 Distribution of missing energies, showing how the two-body  $p + d$  final state can be separated from the three-body  $p + p + n$  final state.

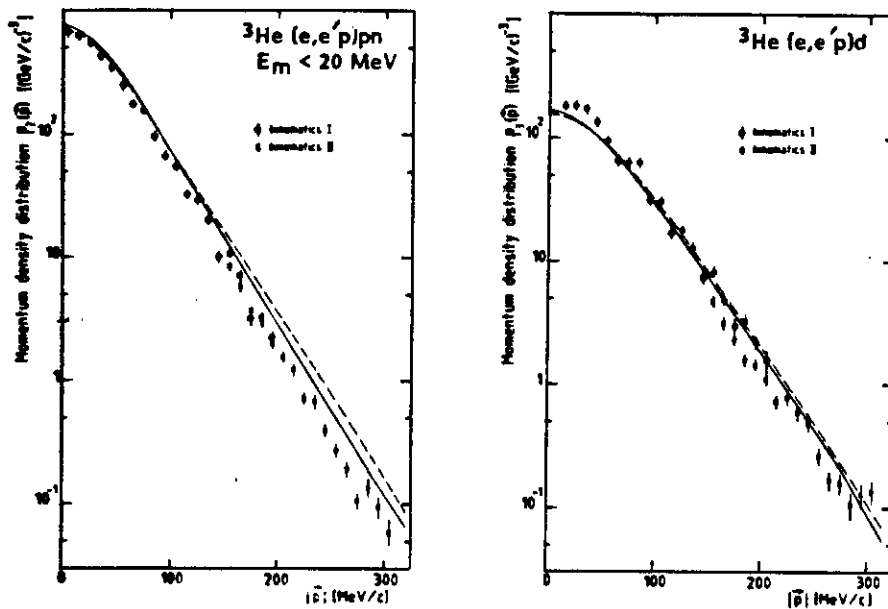


Figure 9 Momentum density distribution for the two-body and the three-body sectors in inelastic electron scattering from  ${}^3\text{He}$ .

undetected, and the target is unpolarized, the cross section can be written

$$\frac{d^6\sigma}{d\Omega dE' d^3p_1} = \frac{\sigma_M}{M_T} \left\{ v_L W_L^{(1)} + v_T W_T^{(1)} + v_{TT} W_{TT}^{(1)} \cos 2\phi_1 \right. \\ \left. + v_{TL} W_{TL}^{(1)} \cos \phi_1 + h v_{TL'} W_{TL'}^{(1)} \sin \phi_1 \right\} \quad (7)$$

where  $\phi_1$  is the out-of-plane scattering angle of the nucleon (as shown in Figure 10),  $h$  is the helicity of the incident electron, and the kinematic factors are

$$v_L = \rho^2 \quad 0 \leq \rho = Q^2/q^2 \leq 1 \\ v_T = \frac{1}{2} \rho + \tan^2 \theta/2 \equiv \frac{1}{2} \rho/\epsilon \\ v_{TT} = -\frac{1}{2} \rho \\ v_{TL} = -\frac{1}{\sqrt{2}} \rho \sqrt{\rho + \tan^2 \theta/2} = -\frac{1}{2} \rho \sqrt{(1 + \epsilon) \rho/\epsilon} \\ v_{TL'} = -\frac{1}{\sqrt{2}} \rho \tan \theta/2 = -\frac{1}{2} \rho \sqrt{(1 - \epsilon) \rho/\epsilon} \quad (8)$$

where  $\epsilon$  is the longitudinal polarization of the virtual photon, and the five  $W_i$  are structure functions that depend on four variables, which can be taken to be  $Q^2$ ,  $\nu$ ,  $p_1$ , and  $\theta_1$ , as shown in Figure 10. An alternative form for Eq. (7) is:

$$\frac{d^6\sigma}{d\Omega dE' d^3p_1} = \Gamma \left\{ \sigma_T + \epsilon \sigma_L + \epsilon \sigma_{TT} \cos 2\phi_1 \right. \\ \left. + \sqrt{\epsilon} (\epsilon + 1) \sigma_{TL} \cos \phi_1 + h \sqrt{\epsilon} (1 - \epsilon) \sigma_{TL'} \sin \phi_1 \right\} \quad (9)$$

where  $\Gamma$  is the virtual photon flux produced by the scattered electron

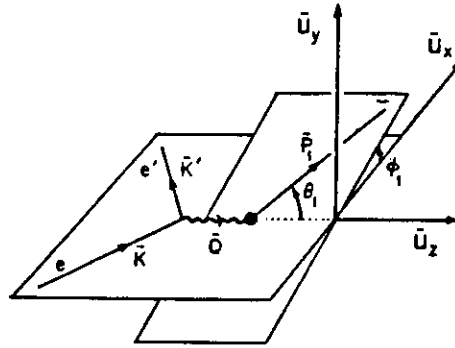
$$\Gamma = \frac{\alpha}{2\pi^2} \left( \frac{E'}{E} \right)^{\frac{1}{2}} \frac{|\vec{q}|}{Q^2 (1 - \epsilon)} = \frac{\sigma_M \rho |\vec{q}|}{4\pi^2 \alpha \epsilon} \quad (10)$$

and

$$\begin{aligned} \sigma_T &= \frac{2\pi^2 \alpha}{M_T |\vec{q}|} W_T^{(1)} \equiv C W_T^{(1)} \\ \sigma_L &= 2\rho C W_L^{(1)} \\ \sigma_{TT} &= -C W_{LL}^{(1)} \\ \sigma_{TL} &= -\sqrt{\rho} C W_{TL}^{(1)} \\ \sigma_{TL'} &= -\sqrt{\rho} C W_{TL'}^{(1)} \end{aligned} \quad (11)$$

Each of these five structure functions or partial cross sections are sensitive to different physical processes. The longitudinal structure function  $W_L$  is sensitive to charge distributions and nuclear wave functions,  $W_T$  is sensitive to magnetic moments, meson exchange currents, and  $\Delta$  processes, and  $W_{TL'}$  is zero without final state interactions. An experimental goal for CEBAF is to separately measure all five of these functions, and to thereby fully determine this important process. To measure  $W_{TT}$  and  $W_{TL'}$  requires measurements out of the  $(e, e')$  reaction plane, but the others can be separated by making measurements at different electron scattering angles (different values of  $\epsilon$ ) and by observing the scattered proton on both the left<sup>n</sup> (where  $\cos \phi_1 = 1$ ) and right<sup>n</sup> (where  $\cos \phi_1 = -1$ ) sides of the three-momentum transfer  $\vec{q}$ .

Figure 10 Exclusive-1 electron scattering. Here the  $z$ -axis is chosen to be along  $q$  and the electron scattering occurs in the  $xz$ -plane. The particle detected in coincidence with the electron has momentum  $p_1$ , whose direction is given by angles  $(\theta_1, \phi_1)$  in this coordinate system.



## 2.2 Two-Nucleon Emission

Two-nucleon knockout,  $(e, e' 2N)$ , can be expected to be sensitive to the pair distribution of nucleons in a nucleus, and to reflect the presence of localized six-quark states as discussed qualitatively in Section 1. Deuteron knockout, a special case, should reflect the existence of pre-existing deuterons or  $^3S$  correlations. However, experience with pion absorption processes where two-nucleon knockout has been extensively studied<sup>16</sup> suggests that final state interactions are very important. One mechanism which seems to occur is  $\Lambda$  excitation, followed by de-excitation through the  $\Lambda N + 2N$  process leading to two-nucleon emission. It is also possible that such processes can generate two  $\Lambda$ 's leading to three- or four-nucleon emission<sup>17</sup>. Very little is known about the electromagnetic two-nucleon knockout process; but studies with electrons, where it is possible to independently vary the energy momentum transfer, and polarization, and to separate a variety of structure functions sensitive to different physical mechanisms (as discussed in Section 2.1) should give much insight into this important process. CEBAF will be an ideal facility at which to carry out such studies.

The  $2p$  knockout reaction is thought to be a promising way to study two-nucleon correlations, since exchange current contributions are strongly suppressed and the  $2p$  system has no dipole moment<sup>18</sup>.

The transverse cross section is therefore expected to be quite small, and the longitudinal cross section should be sensitive to the correlations. However, calculations by Laget<sup>18</sup> suggest that this process is very sensitive to final state interactions. Figure 11 shows the longitudinal ( $\sigma_L$ ) and transverse ( $\sigma_T$ ) cross sections as a

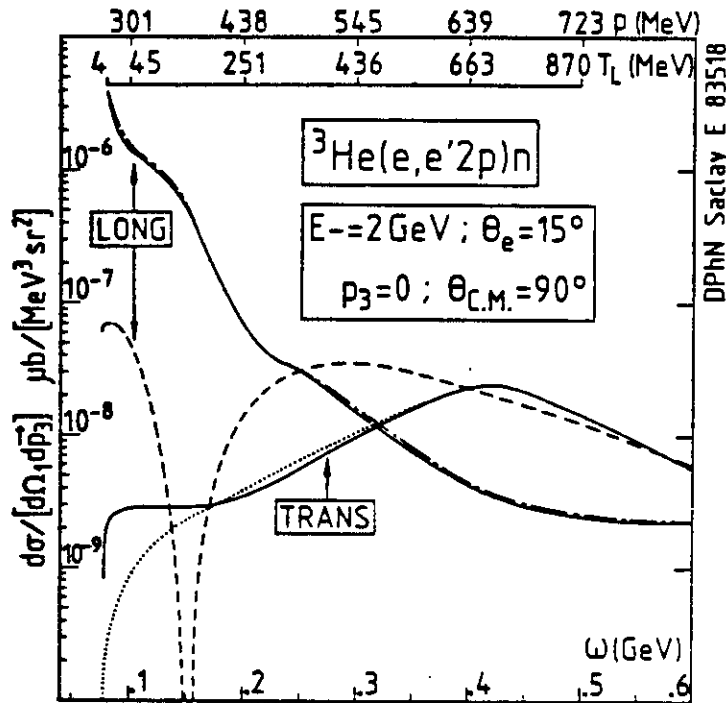


Figure 11 The excitation functions for the transverse and longitudinal cross sections as defined in Eq. (9). Symmetric kinematics with the proton pair initially at rest are assumed. The magnitude of each proton momentum  $p$ , and the relative kinetic energy  $T_L$  are shown along the top axis. Solid curves: full calculations including all final state interactions. Dashed curves: impulse approximation (plane waves in final state) only. Dotted curves: impulse approximation with meson exchange currents.

function of the incoming virtual photon energy  $\omega$  for the case of symmetric kinematics described in Section 2.1 and Figure 4. In the

impulse approximation,  $\sigma_T$  is zero and  $\sigma_L$  shows the oscillatory structure of the initial state correlations clearly. When final state interactions are included, however, the clear connection with initial state correlations is washed out,  $\sigma_L$  can change its value by more than an order of magnitude, and  $\sigma_T$  is no longer zero. More calculations are needed, but it is clear that initial state correlations are only a part of what is happening at lower energies. Things may be simpler at the higher energies accessible to CEBAF where final state interactions are expected to be smaller.

The  $(e, e'np)$  cross section is expected to be larger than the  $(e, e'2p)$  cross sections by at least an order of magnitude, providing a strong incentive for the development of a neutron detection capability to go with this program.

As in the discussion presented in Section 2.1, it may be useful to vary the  $Q^2$  dependence and the  $p^2$  dependence of the cross sections independently. This can be done by using the symmetric kinematics described there, and varying both  $Q^2$  and  $x$  while holding  $p$  constant, or  $p$  and  $x$  while hold  $Q^2$  constant.

### 2.3 Study of Excited Baryons

Measurements of the spectrum of free baryons, together with their electromagnetic and hadronic decay modes, give information essential for constructing and testing realistic quark models of hadrons. Such models are important to nuclear physics for two reasons. First, they provide a bridge between QCD and nuclear structure by providing information and insight needed for the development of models of nuclei based on their underlying quark structure. Secondly, even if the construction of such models is trivial because the effective confinement radius is small and meson theories work for nuclear physics, it is necessary to fully understand the properties of the excited baryons which must necessarily play a role in such a meson theory.

It is also of equally great interest to study the propagation and decay of excited baryons in a nuclear medium, in order to determine  $N^*N$  interaction strengths (where  $N^*$  will be used to denote all excited baryons, including the  $\Delta$  and  $\Lambda^*$ 's) and the effect of the nuclear medium on the structure of the  $N^*$  themselves.

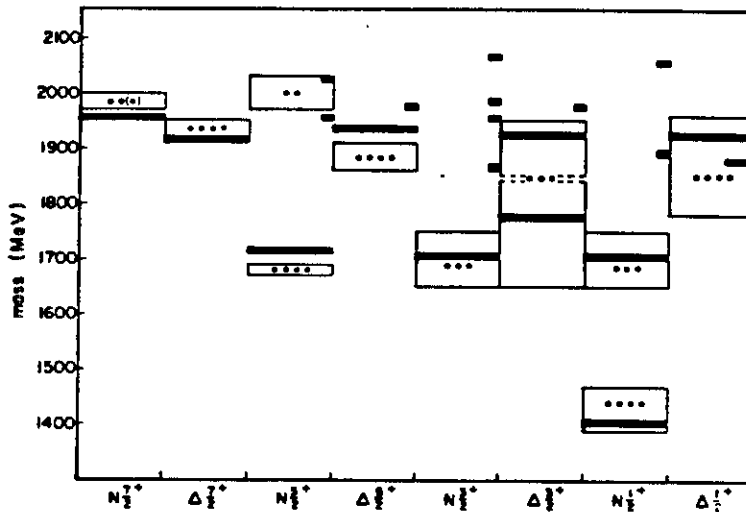
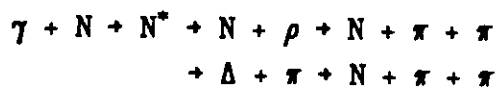


Figure 12 A chart of excited baryons (taken from Ref. 19). The open boxes with asterisks inside correspond to resonances which have been seen in  $\pi N$  scattering (the greater the number of asterisks the more certain are the observations). The solid bars are predictions. The short solid bars label states which are not expected to couple strongly to the  $\pi N$  channel, but could be seen in photoproduction experiments.

Figure 12 shows a table of the predicted and observed lowest lying baryon resonances<sup>19</sup>, all of which can be studied at CEBAF. Note that many have not been seen. This may be due to the fact that they do not appear to couple strongly to the  $\pi N$  channel<sup>20</sup>, which has been the major experimental means of studying baryon resonances. Such resonances can be studied at CEBAF through the reactions



These studies will require a Large Acceptance Spectrometer (LAS) capable of detecting and identifying  $\pi$ 's, K's, and N's over a large

solid angle (80% of  $4\pi$ ). Initial studies will probably be limited to photoproduction measurements, where the goal will be to find the missing states, and to determine their mass and decay widths into  $\gamma N$ ,  $\pi N$ , and  $2\pi N$ . Such studies will be complicated by the fact that the widths of the resonance are expected to be as broad (at least 50 MeV) as the spacing between them, so that they strongly overlap (as shown in Figure 13 (and Figure 19 in Section 2.6 below)). They will have to be separated by a partial wave analysis using a number of the observables which can be measured, including those which depend on polarizations.

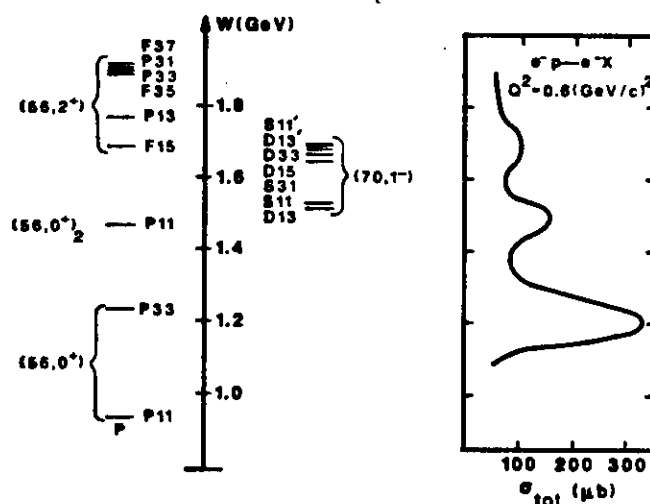


Figure 13 The best known nucleon resonances with masses below 2 GeV (left) and the inclusive electron scattering cross section at  $Q^2 = 0.6 \text{ GeV}^2$  (right). The numbers in brackets indicate the assignments to multiples within the group  $SU(6)_w$ .

CEBAF can also study well established resonances in greater detail than has been possible up until now. The Roper  $P_{11}(1440)$  is an interesting case. While its coupling to real photons is reasonably well known, it has hardly been seen in electron scattering. What data exists suggest that this resonance has a strong coupling to longitudinal photons<sup>21</sup>, a result not obtainable from quark models.

New measurements of the effect of the Roper on electro-production of pions are needed to clarify these issues. It turns out<sup>22</sup> that the production of  $\pi^0$ 's is particularly sensitive to the Roper if the proton target is polarized in a direction transverse to the virtual photon in the electron scattering plane. The expected asymmetry for the process  $\vec{p}(e, e'p)\pi^0$  is shown in Figure 14. Note that  $\phi_1 = \pi/2$ ; the proton must be detected out-of-plane. The VAS spectrometers were designed by V. Burkert for measurements such as these<sup>23</sup>, and with them this program could be readily carried out at CEBAF with a state-of-the-art polarized target.

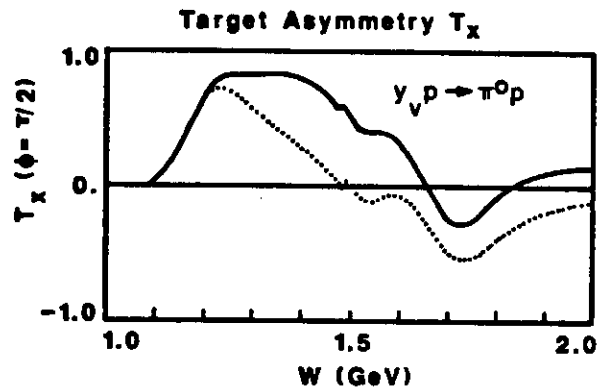


Figure 14 The target asymmetry  $T_x(\phi = \pi/2)$  for single  $\pi^0$  production from protons at  $Q^2 = 1 \text{ GeV}^2$ , and its sensitivity to the  $P_{11}(1440)$  excitation strength. The prediction is based on a recent analysis of DESY and NINA data<sup>21</sup>. Solid line: with  $P_{11}$ ; dotted line: without  $P_{11}$ .

#### 2.4 Hypernuclei - $(e, e'K)$

One of the novel programs proposed for CEBAF is the study of the excitation and decay of hypernuclei by the  $(e, e'K)$  reaction. Hypernuclei are interesting because they contain one strange valence quark, which can be thought of as an impurity in the nuclear system. Study of hypernuclei should give insight into both hyperon-nucleon interactions and nuclear structure.

One system which illustrates how the study of hypernuclei can shed light on fundamental questions is  ${}^4\text{He}$  and  ${}^5\text{He}$  (ref. 24). The  ${}^4\text{He}$  nucleus has 2 neutrons and 2 protons; or 6 valence up and 6 valence down quarks, which completely fill the lowest shell in either the language of nucleons or quarks. Adding a fifth nucleon (neutron) forces all three quarks to occupy the next highest shell, while adding a  $\Lambda$  would require that only the two non-strange quarks occupy the next highest shell, but would allow the strange quark into the lowest shell. In contrast, if the  $\Lambda$  were truly elementary, it could "fully" occupy the lowest shell. This suggests that the behavior of  ${}^5_{\Lambda}\text{He}$  may be sensitive to the underlying quark structure of the  $\Lambda$ , which in this system seems to satisfy a partial exclusion principle. Studies of the level structure and properties of  $\Lambda$  in  ${}^5\text{He}$  may give insight into the underlying quark dynamics.

The  $(e, e'K)$  reaction has several advantages over the more traditional  $(K^-, \pi^-)$  reaction as a means of producing hypernuclei<sup>25</sup>. The electromagnetic process excites both natural and unnatural parity states. Furthermore, since  $K^+$  (or  $K^0$ ) and  $\gamma$  both interact weakly with the nuclear system, these particles can penetrate (or escape from) deep inside of the nuclear medium. This means that the simple impulse mechanism, illustrated in Figure 15, is more likely to describe the reaction than in the  $(K^-, \pi^-)$  case; distorted wave calculations give corrections of a few 10's of a percent for the  $(e, e'K)$  process as opposed to factors of 10 for  $(K^-, \pi^-)$ . It also means that it is possible with  $(e, e'K)$  to convert a proton into  $\Lambda$  deep inside a large nucleus (such as Pb) opening up an entirely new area of study. A disadvantage of the  $(e, e'K)$  process is the energy-momentum mis-match, which means that the momentum transferred to the nucleus cannot be made zero, as in the  $(K^-, \pi^-)$  reaction. However, at high energy the momentum transferred in the  $(e, e'K)$  process can be reduced to a few hundred MeV, favoring transitions in which the angular momentum of the particle is changed by a few units, so that the electromagnetic process naturally favors conversion of a proton in an outer shell into a  $\Lambda$  in an S state.

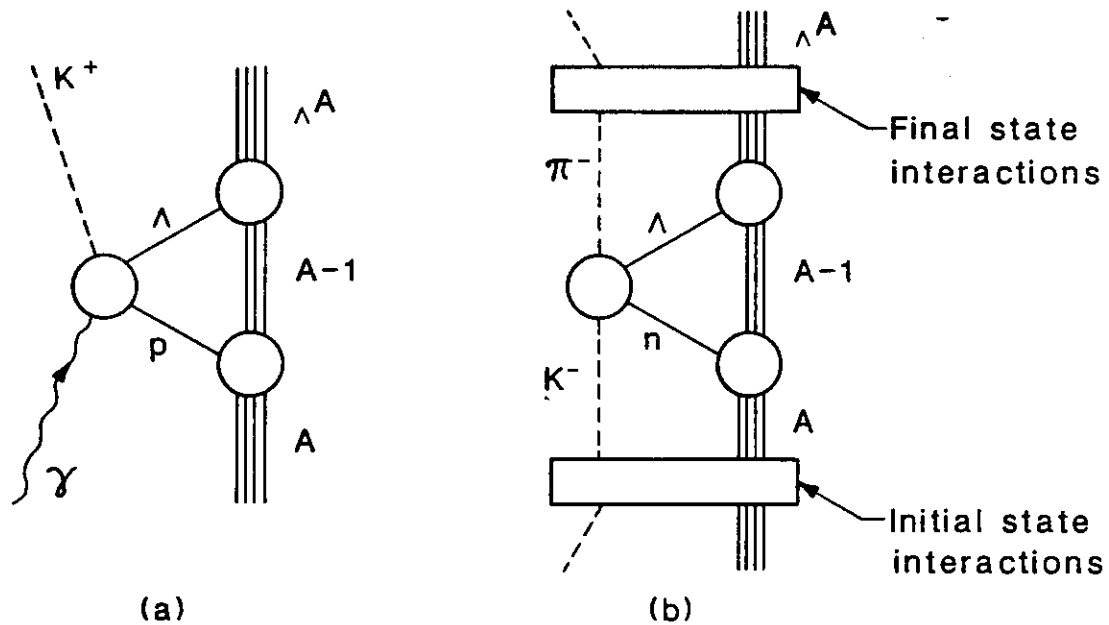


Figure 15 Diagrams showing single-step formation of hypernuclei through  $(e, e'K)$  and  $(K^-, \pi^-)$  reactions. In the  $(K^-, \pi^-)$  case, initial and final state interactions are very strong and cannot be ignored.

Mecking<sup>26</sup> has found that the best way to achieve high resolution and reasonable counting rates in  $(e, e'K)$  is to work in the forward direction, where the electron scattering angle is less than  $1^\circ$  and the kaon angle is  $\leq 5^\circ$ . A possible experimental setup is shown in Figure 16. High resolution is achieved by using an incident electron energy of about 2 GeV, so the outgoing electron has low momentum and can be measured to high precision in a special split-pole spectrometer. The forward kaon can be measured in a high resolution spectrometer, similar (or identical perhaps) to those under consideration for Hall A. If high beam currents and a thin target are used, resolutions of the order of a few 100 keV are possible, and can be improved as the incident beam resolution is reduced below the design value of  $10^{-4}$ . This method is superior to using tagged photons. The resolution expected is 10 times better than that obtainable with  $K^-$  beams.

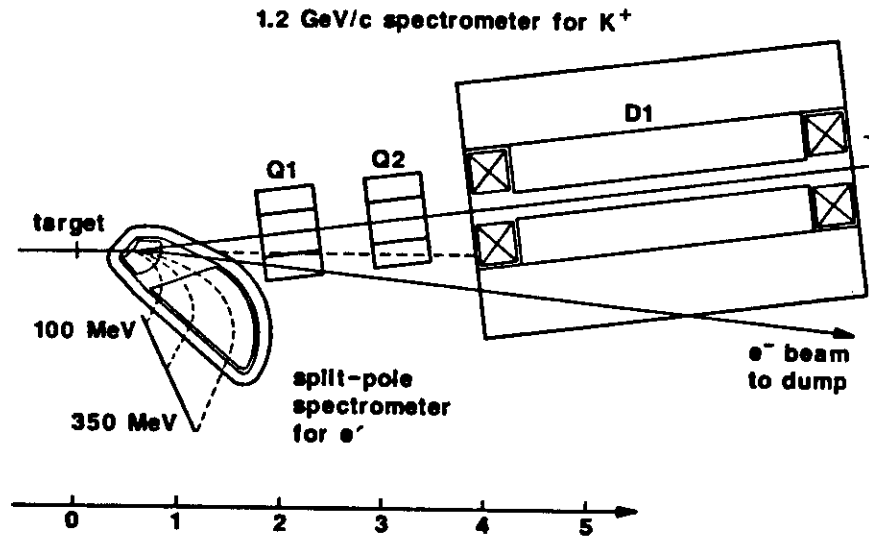


Figure 16 Possible experimental layout for the  $(e, e'K^+)$  program discussed in the text.

## 2.5 Charge Distribution of the Neutron and Deuteron

The charge form factor of the neutron,  $G_{En}$ , is of fundamental importance both because it is sensitive to the distribution of the quarks in its interior, and because it must be taken into account when extracting nuclear structure information from all electron scattering data. Until recently, it has been believed that  $G_{En}$  is small, safely ignorable in all experimental analyses, but a recent attempt by Gari to fit all existing nucleon form factor data<sup>27</sup> has led to speculation that it might be large at  $Q^2 \gtrsim 1 \text{ (GeV/c)}^2$ . If it is large, it may be possible to measure it by separating longitudinal and transverse response functions from  $d(e, e'n)p$  scattering. In any case, use can be made of the CEBAF polarized electron beam to determine  $G_{En}$  in one of two ways:

- the transfer of the electron polarization to the recoiling neutron can be measured in a  $d(\vec{e}, e'n)p$  experiment<sup>28</sup>.
- the target asymmetry for a target polarized transverse to  $\vec{q}$  in the electron scattering plane can be measured in a  $\vec{d}(\vec{e}, e'n)p$  experiment<sup>29</sup>. (Alternatively,  $G_{En}$  may also be measured using polarized  $^3\text{He}$  targets<sup>30</sup>.)

In either case, the experimentally measured quantity is proportional to

$$T = \frac{-2 \sqrt{\tau(1+\tau)} G_M G_E \tan \theta/2}{G_E^2 + G_M^2 + 2(1+\tau)\tau G_M^2 \tan^2 \theta/2} \quad (12)$$

where  $\tau = Q^2/4M^2$ . Hence both the magnitude and sign of  $G_E$  can be obtained directly.

Currently,  $G_{E_n}$  is completely unknown for  $Q^2 \gtrsim 1 \text{ (GeV/c)}^2$ , and the measurements at low  $Q^2$  have large systematic and statistical errors, and are sensitive to the model used for the deuteron wave function, as shown in Figure 17. Precise measurements of  $G_{E_n}$  at both low and high  $Q^2$  are very much needed, and can be done at CEBAF.

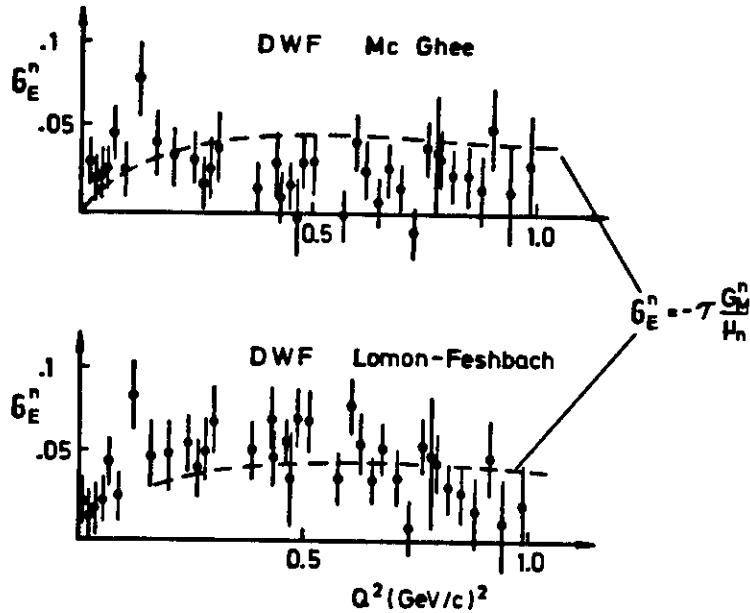


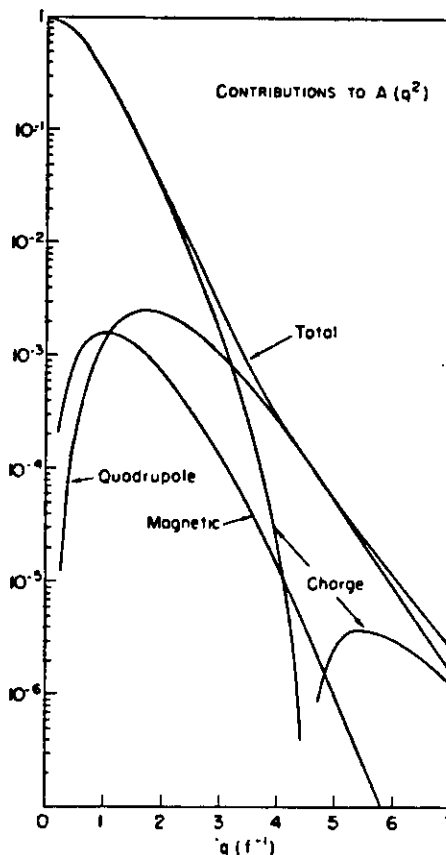
Figure 17 The electric form factor of the neutron derived from elastic electron deuteron scattering for two models of the deuteron wave functions. The results indicate a strong dependence on wave function.

The deuteron charge form factor,  $G_C$ , is also currently unknown. Beautiful high  $Q^2$  measurements of the  $A(Q^2)$  and  $B(Q^2)$  structure functions exist, but from these it is only possible to measure

$$G_C^2 + \frac{8}{9} \eta^2 G_Q^2 = A(Q^2) - \frac{B(Q^2)}{2(1 + \eta)} \quad (13)$$

where  $G_Q$  is the quadrupole form factor and  $\eta = Q^2/4M_d^2$ . Unfortunately, much of the nuclear structure is washed out by this combination of form factors, as shown in Figure 18. A separate determination of  $G_C$ , particularly near its predicted zero, would be a sensitive indicator of short range structure, relativistic and meson exchange effects, and quark degrees of freedom.

Figure 18 Contributions to the A structure function of the deuteron from the charge,  $G_C^2$ , quadrupole,  $8/9\eta^2 G_Q^2$ , and magnetic terms for a typical model. Note the zero in  $G_C^2$  near  $Q^2 \approx 0.85 \text{ (GeV/c)}^2$  is completely obscured by quadrupole terms.



As for the neutron, a vector polarization transfer can be measured with a polarized electron beam, or, alternatively,

asymmetries due to tensor polarization can be measured with unpolarized electron beams<sup>28</sup>. From these asymmetries  $G_C$  and  $G_Q$  can be separated. Measurements of  $T_{20}$  have already been carried out at Bates and Bonn, but at momentum transfers well below the region where  $G_C^2$  has its minimum<sup>31</sup>. A new experiment is planned for Bates, which should probe  $T_{20}$  near  $Q^2 = 1 \text{ (GeV/c)}^2$ , a very interesting region. At CEBAF, better measurements at lower and higher momentum transfers will be possible.

## 2.6 Studies in the Deep Inelastic Region

Inclusive measurements of electron and muon scattering,  $(e, e')$  and  $(\mu, \mu')$ , have provided some of the best information about quarks. When analyzed in conjunctions with neutrino and antineutrino charge changing reactions  $(\nu, \mu^-)$  and  $(\bar{\nu}, \mu^+)$ , they give an explanation of the data in terms of lepton scattering from individual quarks, yielding an almost model independent determination of the number of valence quarks, the distribution functions for valence and ocean quarks, the percentage of momentum carried by gluons, and the rms charge carried by the quarks<sup>32</sup>. And the EMC effect, which has generated such interest, gives information about quark distributions in nuclei, regardless of which explanation eventually prevails.

In view of the success of the quark description of inclusive scattering in the deep inelastic region, it is particularly interesting to see whether or not some of this success can be extended to the description of the behavior of exclusive channels such as  $(e, e' \pi)$ ,  $(e, e' 2\pi)$ ,  $(e, e' K)$  and other processes. How is the total cross section built up out of these individual channels, and how does this composition change as one moves deeper into the scaling region? Specific questions that could be addressed in an initial program of CEBAF experiments are the study of the A dependence of single hadron production, measurement of the ratio of positive to negative hadron production which may be sensitive to differences in densities of ocean  $u\bar{u}$ ,  $d\bar{d}$ , and  $s\bar{s}$  quarks, and studies of the  $Q^2$ ,  $x$ , high  $p$  and  $\phi$  dependencies of single hadron

production. A list of specific experiments of interest was developed at this Workshop by the working group on this topic and is summarized in Karl Van Bibber's report<sup>33</sup>.

CEBAF's 4 GeV design energy was chosen to permit a complete study of the proton (and hence nucleus) inelastic structure functions from the region where resonances and other effects of collective quark structure are visible, up to the onset of deep inelastic scattering, where the structure functions become a function only of the Bjorken x-scaling variable, Eq. (5), and inclusive scattering is described by incoherent scattering from point-like quarks. Figure 19 shows the kinematic region which can be explored by a 4 GeV and a 6 GeV accelerator. The 4 GeV accelerator can cover the transition region, as was intended, but cannot carry on a very extensive program in the deep inelastic region. Extending the energy to 6 GeV, which appears to be a likely possibility if the superconducting cavities continue to exceed specifications (as described in the overview report with this proceedings), will considerably expand the possible program of deep inelastic studies, and further increases in energy will help still more.

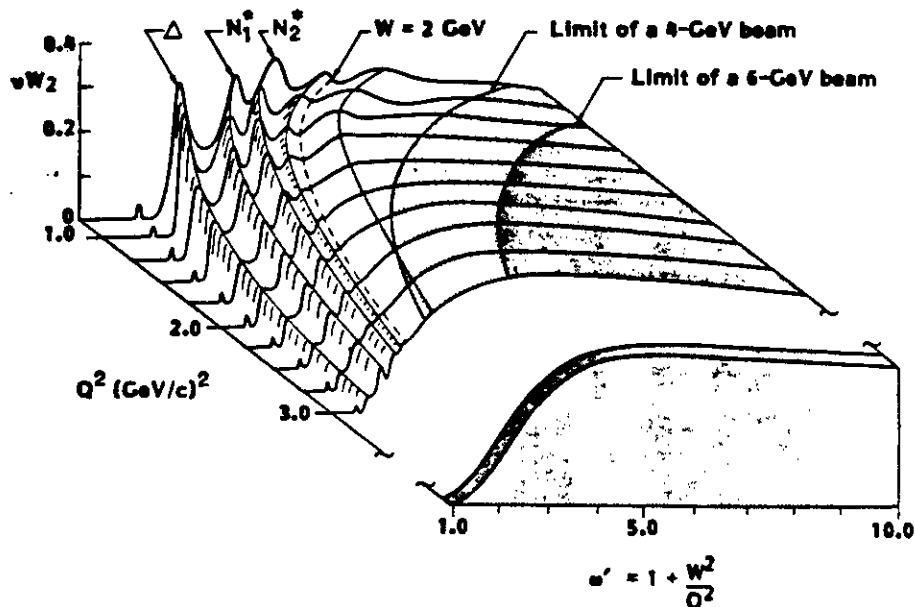


Figure 19 The proton inelastic structure function  $vW_2$  shown as a function of  $Q^2$  and the scaling variable  $w'$ . The regions which can be studied by a 4-GeV accelerator and a 6-GeV accelerator lie to the left of the limits shown.

## 2.7 Studies of the Electroweak Interaction

The weak neutral current can be studied by measuring the parity violating asymmetries

$$A = \frac{\sigma_+ - \sigma_-}{\sigma_+ + \sigma_-} \quad (14)$$

for the scattering of electrons with positive and negative helicity. This asymmetry measures the interference between the electromagnetic interaction and the parity violating parts of the weak neutral interaction, which arises from the exchange of a  $Z_0$  boson. Assuming the electromagnetic interaction is known, precision measurements of  $A$  can be converted into precision measurements of the coupling constants of the  $Z$  boson to the constituent quarks in various nuclear targets. By selecting the quantum numbers of the initial and final hadronic states, and choosing different electron scattering angles, different combinations of these coupling constants can be isolated and measured. While the standard model gives all of these coupling constants in terms of only one parameter,  $\sin^2\theta_w$ , which has been measured to about 5%, it is important to test this model to the highest possible precision. Tests of semi-leptonic processes inside the nuclear medium, where the strong interactions are strong and confining, are particularly valuable.

Elastic scattering from the proton and  $\Delta^+$  production both have large cross sections, and have been proposed as a test of the electroweak theory which could be carried out at CEBAF<sup>34</sup>. The general interaction of the  $Z_0$  with  $u$  and  $d$  quarks can be expressed in terms of four constants,  $\alpha$ ,  $\beta$ ,  $\gamma$  and  $\delta$ . Only  $\gamma$  will be measured in the Bates asymmetry experiment on carbon, and the SLAC experiment was dominated by  $\alpha$ <sup>35</sup>. Elastic measurements from the proton will give information about all 4 constants, but are more sensitive to  $\gamma$  and  $\beta$ , depending on the scattering angle. The reaction  $e p \rightarrow e' \Delta^+$  depends on  $\alpha$  and  $\beta$  only, and this measurement would therefore help to separate  $\alpha$ ,  $\beta$  and  $\gamma$ .

CEBAF's 100% duty factor will be helpful to this program by permitting instantaneous rates to be lowered to a level where individual pulses can be counted<sup>34</sup>. The asymmetries to be measured are of the order of  $10^{-5}$ , and hence systematic errors must be lowered to the  $10^{-7}$  level to permit the 1% measurements required for precision tests. If the systematic errors can be reduced sufficiently, and special targets capable of taking high beam currents are available, it is estimated<sup>34</sup> that data for the needed 1% statistical accuracy can be accumulated in 100's of hours.

### 3. Experimental Requirements for the Planned Program

CEBAF will be equipped with three experimental halls, designated A, B, and C. While the mission of each of these halls is being currently worked out, and will probably undergo further evolutionary changes in the months ahead, the major function of each hall has already emerged, at least in broad outline, and will be summarized briefly. For a detailed discussion of each of the Halls, with a description of the equipment planned or under consideration, see the following talk by J. Mougey.

- Hall A will be devoted to studies where high momentum and angular resolution are needed. This will include single nucleon knockout  $A(e, e'N)A-1$ , and studies of hypernuclei  $A(e, e'K)_{\Lambda}A$ , where a resolution of  $\sim 200$  keV is needed to separate closely spaced nucleon levels. Studies of the  $(e, e'N)$  reaction from few body systems, which require resolutions of about 1 MeV, will also have to be done in this hall. It is desirable that the spectrometers in Hall A be able to move over the widest possible angles, and be capable of making out-of-plane measurements so that the individual structure functions can be fully separated. It should also be possible to use polarized targets, and detect neutrons in Hall A.

- Hall C will be devoted to the study of correlated, few particle final states in cases where it is desirable to trade

high resolution for large angular and momentum acceptance. It seems likely that resolutions of a few to 10 MeV are the best that will be achievable in this hall, but angular acceptances of up to 50 msr and momentum bites of a factor of 2-3 will be gained as a consequence, at least for the proposed VAS hadronic spectrometer. This hall is the likely home of  $(e, e'2N)$  measurements, and will also be ideal for the study of baryon resonances in cases where specific signatures are sought after, as in the case of the Roper described in Section 2.3. As in Hall A, motion of spectrometers through the widest possible angular range, out-of-plane capability, ability to detect neutrons, and ability to use polarized targets are all needed. In addition, this may be the hall where a program of triple coincidence measurements is most likely to begin, and measurements of  $G_{En}$  and  $G_C/G_q$  carried out.

- Hall B will be devoted to the study of uncorrelated, many particle final states, where large nearly  $4\pi$  acceptance is essential and 1% resolution is acceptable, and to tagged photon studies where large acceptance is needed to compensate for a low photon flux. It also will be an ideal place to initiate new programs (such as two-nucleon knockout) where a broad exploration of the phase space is needed before focusing in detail on specific processes or choices of kinematics. It will probably be the major home for studies of excited baryons and exclusive processes in the deep inelastic, x-scaling region. To achieve the needed  $4\pi$  acceptance, a large acceptance spectrometer (LAS) is being developed. Finally, to allow for the possibility that parity studies may be carried out in Hall B, it will be designed, together with Halls A and C, to handle the full beam intensity.

To design and build equipment to carry out this exciting program, to keep within the budget allocated to experimental equipment, and to have the equipment ready by 1992 will be a major challenge. CEBAF looks toward its user Community to help and to contribute to this exciting endeavor.

## References

1. See, for example, "A Long Range Plan for Nuclear Science", a report by NSAC, 1983; Report of the NSAC Subcommittee on Facility Construction, 1986.
2. See, for example, T. DeGrand, et al., Phys. Rev. D 12, 2060 (1975).
3. E. Witten, Nucl. Phys. B160, 57 (1979).
4. See, for example, I. Zahed and G.E. Brown, Phys. Rep. 142 1 (1986).
5. A.W. Thomas, Adv. Nucl. Phys. 13, 1 (1984); G.A. Miller, Int. Rev. Nucl. Phys. 2 (1984).
6. See, for example, D. Robson, Prog. Part. Nucl. Phys. 8, 257 (1982); M. Oka and K. Yazaki, Int. Rev. Nucl. Phys. I, 489 (1984); C.W. Wong, invited talk given at the European Workshop on Few-Body Physics, Rome, Italy, October 1986, to be published.
7. "Research Program at CEBAF", the report of the CEBAF 1985 Summer Study Group, referred to as RPAC, published by CEBAF.
8. See the SURA 1980 and 1982 NEAL (now called CEBAF) proposals.
9. See the Report of the Workshop on Future Directions in Electromagnetic Nuclear Physics, 1981, organized and published by the Bates (MIT) User's Group.
10. W.W. Buck and F. Gross, Phys. Rev. D 20, 2361 (1979).
11. P. DeWitt-Huberts, invited talk presented at the XI Europhysics Divisional Conference, Paris, July 1985, published in the proceedings, Nucl. Phys. A446, 301c (1985).
12. M. Bernheim, et al., Nucl. Phys. A365, 349 (1981).
13. E. Jans, et al., Phys. Rev. Lett. 49, 974 (1982).
14. H. Arenhovel, Nucl. Phys. A384, 287 (1982) and S. Frullani and J. Mougey, Advances in Nucl. Phys. 14 (1984).
15. T.W. Donnelly, Proc. of the CEBAF 1985 Summer Workshop, p. 57.
16. A. Altman, et al., Phys. Rev. Lett. 50, 1187 (1983); Phys. Rev. C, to be published; P.G. Roos, invited talk present at this workshop and included in these proceedings.

17. E. Oset, Y. Futami, and H. Toki, Nucl. Phys. A448, 597 (1986); J.P. Schiffer, Comments on Nucl. and Part. Phys. 14, 15 (1985).
18. J.M. Laget, Phys. Lett. 151B, 325 (1985); Saclay preprint DPh-N/no 2367, 1986.
19. R. Koniuk and N. Isgur, Phys. Rev. D21, 1868 (1980).
20. N. Isgur, Proc. of the CEBAF 1984 Summer Workshop, p. 199.
21. G. Kroesen, Diploma Thesis, Bonn (1983), unpublished.
22. V. Burkert, Ref. 7, p. 5-1.
23. V. Burkert, *ibid*, p. 11-54.
24. E. V. Hungerford and L.C. Biedenharn, Phys. Lett. 142B, 232 (1984); Y. Kurihara, Y. Akushi, and H. Tanaka, Phys. Rev. C31, 971 (1985); T. Yamazaki, invited talk at the XI International Conference on Few Body Systems, Tokyo, Aug. 1986, to be published in the proceedings.
25. T.W. Donnelly and S.R. Cotanch, Ref. 7, p. 7-1.
26. B.A. Mecking, Ref. 7, p. 7-25.
27. M. Gari and W. Krumpelmann, Z. Phys. A322, 689 (1986).
28. R.G. Arnold, C.E. Carlson, and F. Gross, Phys. Rev. C23, 363 (1981).
29. See V. Burkert, Ref. 7, p. 9-1.
30. R.D. McKeown and R.G. Milner, Ref. 7, p. 12-45; B. Blankleider and R.M. Woloshyn, Phys. Rev. C29, 538 (1984).
31. M.E. Schulze, *et al.*, Phys. Rev. Lett. 52, 597 (1984).
32. See, for example, A. Benvenuti, *et al.*, Phys. Rev. Lett. 42, 1317 (1979).
33. K. van Bibber, report of working group E, published in these proceedings.
34. P.A. Souder, *et al.*, SURA 1982 NEAL proposal, p. A-237 and Ref. 9, p. 385.
35. C.Y. Prescott, *et al.*, Phys. Lett. B84, 524 (1979).